

Schaufele Annotations

Chapter 1 Review of Basic Concepts

The Airplane in Motion

Three airplane orthogonal axis systems are commonly in use with the following characteristics:

1. Drawing axis system (Figure 1.1)
 - Origin forward of the nose and below the aircraft (so that x- and z-values are always positive)
 - X-axis facing aft along some reference line (sometimes the static ground line, sometimes the passenger cabin line)
 - Y-axis facing to starboard and horizontal
 - Z-axis facing up.
2. Wind axis system (used for aircraft performance)
 - Origin at center of gravity
 - X-axis pointing into apparent wind
 - Y-axis pointing horizontally to starboard
 - Z-axis pointing down.
3. Stability axis system (used for stability and control analysis)
 - Origin at center of gravity
 - X-axis pointing into apparent wind in side elevation (Schaufele Figure 1-2), pointing along aircraft axis of symmetry in plan view (Schaufele Figure 1-3)
 - Y-axis pointing horizontally to starboard
 - Z-axis pointing down.

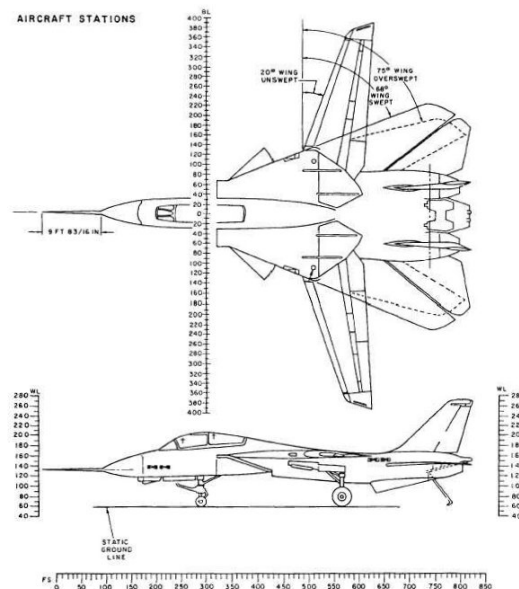


Figure 1.1 Example of Drawing Axis System

Airplane drafting uses some terms that are adapted from naval architecture. In the drawing axis system the airplane may commonly be sectioned in three planes:

1. Y-Z plane: Sections are usually called fuselage stations (abbreviated as FS, see Figure 1-1), and the term is also applied to the cutting plane itself, as it is for the other two cutting planes.
2. X-Z plane: Sections of the outer mold line (OML) are called buttock (or butt) lines (abbreviated as BL).
3. Y-X plane: Sections of the OML are called waterlines (abbreviated as WL).

For supersonic-cruise airplanes, other cutting planes may be used, such as those lying on the Mach lines at the cruise condition.

The wing may also have its own set of reference axes. The issue is compounded by the fact that the wing is flexible, and the shape of the wing is determined by the g-loading, aerodynamic loading and amount of fuel in the wing.

In the stability axis system, the inconsistency in the way that the X-axis is defined between the horizontal and vertical planes (pointing into the apparent wind in side elevation, but attached to the airplane in plan view), results in a similar inconsistency in the sign of stable static stability derivatives. In pitch, C_{m_α} must be negative for a stable configuration, whereas in yaw C_{n_β} must be positive for stability.

For aerodynamic analysis, forces and moments may be referenced to the wing section quarter-chord for wing section data, or the quarter-chord of the mean aerodynamic chord (m.a.c.) for wing data. This is usually very close to the section or wing aerodynamic center. It may also be used as the origin for airplane reference axes, because for an airplane with a conventionally-located horizontal stabilizer, the reference center of gravity is often located close to the wing quarter-chord. This will be discussed in more detail in Chapter 4.

Airplane Drag Curve (Drag Polars)

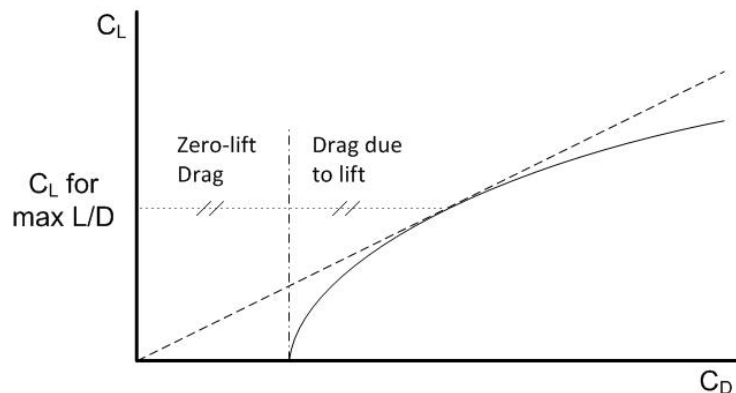


Figure 1.2 Calculating C_L at Maximum Lift/Drag Ratio

Ignoring compressibility effects, an aircraft drag polar (Figure 1.2) may be approximated as:

$$C_D = C_{D_0} + K C_L^2 \quad \text{Eq. 1.1}$$

The point on the polar where C_L/C_D is maximized is where the tangent from the origin touches the curve, i.e., where the gradient of the tangent from the origin equals the gradient of the curve. Thus:

$$\frac{C_D}{C_L} = \frac{dC_D}{dC_L} \quad \text{Eq. 1.2}$$

$$\text{Differentiating Eq. 1.1: } \frac{dC_D}{dC_L} = 2KC_L \quad \text{Eq. 1.3}$$

$$\text{Thus } \frac{C_D}{C_L} = 2KC_L \text{ or } C_D = 2KC_L^2 \quad \text{Eq. 1.4}$$

Inserting this back into Eq. 1.1 we have $C_{D_0} = KC_L^2$, i.e., at the location on the polar where C_L/C_D is maximized, zero-lift drag is equal to drag due to lift.

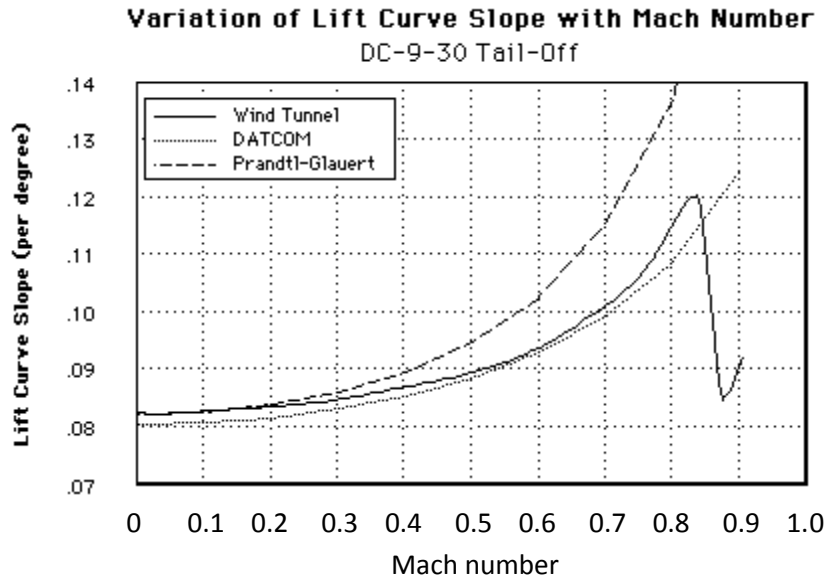
$$\text{For the condition of maximum L/D: } C_L = \sqrt{\frac{C_{D_0}}{K}} \quad \text{Eq. 1.5}$$

$$\text{and } \left(\frac{L}{D}\right)_{\max} = \frac{1}{2\sqrt{KC_{D_0}}} \quad \text{Eq. 1.6}$$

This is the condition for optimum endurance (e.g., when loitering), and related to the condition for maximum range, which is usually at a slightly lower C_L for which $\frac{L}{D} = 0.866\left(\frac{L}{D}\right)_{\max}$. This latter condition arises from the requirement to maximize $V(L/D)$ in the Breguet range equation, which will be discussed in a later chapter.

Mach Number Effects on Lift and Drag Curves

On page 22 Schaufele states that the gradient of the lift curve increases with Mach number by a factor of $\frac{1}{\sqrt{1-M^2}}$ (the Prandtl-Glauert transformation), where M is the free-stream Mach number. This is true of a wing section, but not for a wing, and then only up to about $M = 0.8$. For a swept wing, the increase in the gradient of the lift curve is only about 60% of the value predicted by the Prandtl-Glauert transformation, as shown in Fig. 1.3. The DATCOM (Ref. 1.1) value is much closer to the experimental data.



Source: Ilan Kroo

Figure 1.3 Comparison of Calculated and Experimental $C_{L\alpha}$

Schaufele references Figures 1-25 through 1-27 in the context of airplanes that are designed to operate at supersonic speeds. However, the curves shown here are more appropriate for a high-subsonic design. For an airplane designed for supersonic cruise the change in slope of the curves around Mach 0.95 is spread out over a wider Mach range, from Mach 0.95 to Mach 1.2 or so, depending on the design.

References

- 1.1 Hoak, D.E., "The USAF Stability and Control DATCOM", Air Force Wright Aeronautical Laboratories, TR-83-3048, Oct 1960